Evolution of the global wind wave climate in CMIP5 experiments

M. Dobrynin,[1,2] J. Murawsky,[1] and S. Yang[1]

Received 26 June 2012; revised 14 August 2012; accepted 15 August 2012; published 22 September 2012.

[1] Ocean wind waves follow shifts in atmospheric circulation and wind regimes caused by climate change and variability. We use a wave model (WAM) forced by winds from an Earth system model (EC-Earth) to study the evolution of global wave climate in terms of trends in wind speed and wave height, their rates and anomalies over the 250 years. Historical period and future scenarios (RCP8.5 and RCP4.5) are calculated within the fifth phase of the Coupled Model Intercomparison Project. Both scenarios indicate a future increase of wind speed and wave height in the Arctic and Southern Ocean and a decrease in the Pacific Ocean. Some regions, e.g., the North Atlantic show a change of sign from currently positive to negative trends in this century. Swell dominated regions, connected to the Southern Ocean show opposite trends for winds and waves. Calculated trends are evaluated taking into account natural variability estimated from a simulation with pre–industrial climate. We conclude that projected wave heights are still within natural variability, whereas wind speed exceeds it in the Arctic and Southern Ocean. Probability estimates show that extreme winds and waves become more dominant in the Southern Hemisphere, Arctic and Indian Ocean. Low and medium winds and waves are highly probable in the North and Equatorial Atlantic and Pacific. **Citation:** Dobrynin, M., J. Murawsky, and S. Yang (2012), Evolution of the global wind wave climate in CMIP5 experiments, *Geophys. Res. Lett.*, *39*, L18606, doi:10.1029/2012GL052843.

1. Introduction

[2] Atmospheric circulation regimes adapt to climate change [*Intergovernmental Panel on Climate Change*, 2007] with a different intensity around the Earth [*Marshall*, 2003; *Shindell and Schmidt*, 2004; *Lorenz and DeWeaver*, 2007; *Woollings et al.*, 2012]. Having the wind as a major forcing factor for the surface waves and considering the changes in the atmospheric circulation, we are to expect changes in wave regime in line with the changes of wind distribution over the globe. Wind and wind waves are key factors that have strong impacts on the exchange of energy and momentum between the atmosphere and the ocean [*Donelan et al.*, 1997] and influence the mixing of upper ocean [*Babanin*, 2006; *Babanin et al.*, 2009; *Pleskachevsky et al.*, 2011; *Qiao and Huang*, 2012]. Results from many studies show the measured [*Carter and Draper*, 1988; *Bacon and Carter*, 1991; *Allan and Komar*, 2000; *Young et al.*, 2011] or modeled [*Cox and Swail*, 2001; *Wang and Swail*, 2006] trends in wind speed and significant wave height in different regions. Commonly, the analysis of trends is limited by geographical or temporal availability of data, either observations or forcing data for model simulations. Therefore, reported trends refer often to limited periods of time, typically a few decades and most often focus on specific regions. On the longer time scale, these trends may be a part of inter-decadal climate variability. Analysis of winds and waves in a simulation over hundreds of years helps us to understand the nature of trends and its variability. Presented here is the analysis of modeled wind and waves which covers the entire 250 years period of the fifth phase of Coupled Model Intercomparison Project (CMIP5) simulations, highlighting different trends globally and on the regional scale of ocean basins [*Levitus et al.*, 2006].

2. Global Wave Climate Modeling

[3] We used the 3rd generation spectral wave model WAM [*Wamdi Group*, 1988] forced by historical and future winds simulated by the Earth system model EC-Earth [*Hazeleger et al.*, 2012] in the CMIP5 experiments.

[4] Calculated wave spectra cover the logarithmically scaled wave frequency range of 32 bands from 0.042 Hz to 0.802 Hz, and 24 directions (15° resolution) from 7.5° to 325.5° on a staggered angular grid, shifted by half the directional increment to the cardinal directions. Latter shall prevent extensive wave growth along the grid axes of the spatial representation. The wave model runs in shallow water mode on a global, spherical grid with a resolution of 1° and the topography based on the ETOPO1 [*Amante and Eakins*, 2009]. North Pole and fast ice covered regions north of 84° have been taken out of the analysis. Capillary waves have been implemented as a lower spectral energy limiter, corresponding to 7×10^{-2} m wave height. This enhances wave growth from calm sea.

[5] The EC-Earth model used in CMIP5 experiments consists of atmospheric and ocean components, i.e., the Integrated Forecast System (IFS) of the European Centre for Medium Range Weather Forecasts (ECMWF) and the Nucleus for European Modelling of the Ocean (NEMO) developed by Institute Pierre et Simon Laplace (IPSL), which is coupled to the Louvain-la-Neuve sea Ice Model (LIM) embedded in NEMO. All atmospheric and ocean modules are coupled by the OASIS3 software. The atmospheric component is configured at T159 horizontal spectral resolutions (equivalent to 125 km × 125 km) and 62 vertical levels, while the ocean component has a horizontal resolution of 1° × 1° with a refinement of 1/3° in the tropics and 42 vertical levels. To assess natural variability, surface winds from a 350 years EC-Earth simulation under pre-industrial conditions (hereafter referred to as control run) were analyzed and used as reference state. The EC-Earth simulations are following the CMIP5 protocol for long-term simulations [*Taylor et al.*,

[1]Danish Meteorological Institute, Copenhagen, Denmark.
[2]Now at Institute of Oceanography, University of Hamburg, Hamburg, Germany.

Corresponding author: M. Dobrynin, Institute of Oceanography, University of Hamburg, Bundesstraße 53, D-20146 Hamburg, Germany. (mikhail.dobrynin@zmaw.de)

0094-8276/12/2012GL052843

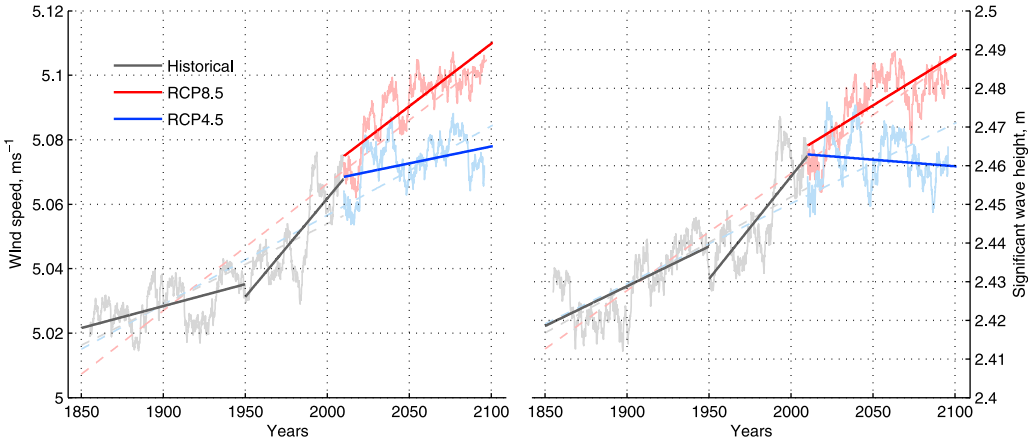

Figure 1. Projected global trends in (left) wind speed (ms^{-1}) and (right) significant wave height (m) for the historical period of 1850–2010 (grey dash lines); two historical sub-periods of 1850–1950 and 1950–2010 (black lines); the future period of 2010–2100 for scenarios RCP8.5 (red lines) and RCP4.5 (blue line); and the whole period of 1850–2100 with scenarios RCP8.5 (dashed red line) and RCP4.5 (dashed blue lines). Shadowed lines are 10 year running mean values.

2012], which was implemented for the historical period of 1850 to 2005 and for the continuing future period of 2006 to 2100 for the two scenarios RCP8.5 and RCP4.5 [*van Vuuren et al.*, 2011]. Here, the historical experiment, initialized from the control run, uses climate forcing (i.e., solar forcing, GHGs, ozone and aerosol concentrations and historical land-used) starting from 1850. The ocean and atmospheric circulations are then developed according to the model internal dynamics and physics with no other constrains. For reasons of convenience we extend the historical period until 2009 using RCP4.5 data for the period 2006–2009, as CMIP5 suggested. The future period starts therefore at 2010.

[6] The WAM model was forced by EC-Earth 3 hourly wind data and has been "cold started" in 1850 for the historic assessment and in 2010 for future projections using fully developed sea. We have calculated the historical wave climate on the extended time scale for the historical period from 1850 to 2010 and for the future projections until 2100 for two scenarios RCP8.5 and RCP4.5.

3. Global Trends in Surface Wind Speed and Significant Wave Height

[7] Over the entire period of simulation from 1850 to 2100 for both scenarios RCP8.5 and RCP4.5 [*van Vuuren et al.*, 2011], we project a continuous rise of globally monthly averaged significant wave height with decadal oscillations accompanied by an increase of wind speed over sea. This increase is calculated from a linear trend in the wind speed and wave height at the end of 2100 (Figure 1). The change of global mean significant wave height over the 250 years is 0.07 m or 3.14% relative to 1850 for RCP8.5 and 0.05 m or 2.14% for RCP4.5. The increase in wind speed is 0.72 ms^{-1} (2.0%) for RCP8.5 and 0.55 ms^{-1} (1.8%) for RCP4.5, in comparison to the year 1850. For the historical period (1850–2010) the increase was 0.03 m (1.55%) for wave height and 0.04 ms^{-1} (0.80%) for wind speed. We calculate the natural variability as the standard deviation of the control run for wind speed (0.28 ms^{-1}) and the historical run for wave height (0.11 m). That means in fact that the estimated value for wave height includes natural variability as well as external changes. However, it provides to a large degree a good estimate of the natural variability, since anthropogenic forcing is rather weak or at a moderate level during large parts of the historical period. The above trends in the globally averaged wind speed and wave height are within the range of the variability of the model.

[8] The rate of the trends is not constant over the period of simulation. We introduced three periods: the first part of historical run from 1850 to 1950, second, from 1950 to 2010 and the future period from 2010 to 2100. We found that the largest rate of increase occurred in the second period from 1950 to 2010, with an increase rate of 0.54×10^{-2} m per decade for the wave height and 0.62×10^{-2} ms^{-1} per decade for the wind speed (Figure 1 and Table 1). This exceeds the rate of 0.21×10^{-2} m per decade for the wave height and 0.14×10^{-2} ms^{-1} per decade for the wind speed in the previous period (1850 to 1950) by approximately a factor of four for wind speed and three for wave height. The future wind wave climate is predicted as an increase of 0.26×10^{-2} m per decade (RCP8.5) and a negligible decrease of -0.04×10^{-2} m per decade (RCP4.5), which is accompanied by a wind speed increase of 0.39×10^{-2} m and 0.11×10^{-2} ms^{-1} per decade for RCP8.5 and RCP4.5 respectively. We refer these changes in trends and rates to the long-term variations of atmospheric circulation regimes, such as polewards shift of jets and intensified polar winds [*Yin*, 2005; *Lorenz and DeWeaver*, 2007; *Woollings et al.*, 2012].

4. Anomalies, Trends and Shifts in Regional Wind and Waves Regimes

[9] We have calculated relative anomalies and linear trends in wind speed and wave height for the last decade of 20th and 21st centuries, in order to highlight most significant changes in various ocean basins [*Levitus et al.*, 2006] as projected in our experiments (Figures 2 and 3). The mean values from the period from 1850 to 1870 have been used as a reference.

[10] We used altimeter data of monthly mean significant wave height provided by *Zieger et al.* [2009] for comparison with the WAM model (Figure S1 in the auxiliary material).[1]

[1]Auxiliary materials are available in the HTML. doi:10.1029/2012GL052843.

Table 1. Linear Trends in the Wind Speed (W) in $ms^{-1} \times 10^{-2}$ per Decade and Significant Wave Height (Hs) in $m \times 10^{-2}$ per Decade and Their Variability (in $ms^{-1} \times 10^{-2}$ and $m \times 10^{-2}$, Respectively)[a]

	1850–1950		1950–2010		2010–2100 RCP8.5		2010–2100 RCP4.5		Variability	
Region	W	Hs	W	Hs	W	Hs	W	Hs	W[b]	Hs[c]
Arctic Ocean	0.31 (3)	0.06 (1)	2.27 (13)	0.59 (3)	6.69 (60)	2.18 (20)	4.58 (41)	1.43 (13)	42	25
Indian Ocean	−0.05 (−1)	0.17 (2)	0.13 (1)	0.78 (5)	−1.08 (−10)	0.13 (1)	−0.42 (−4)	0.07 (1)	46	44
Southern Ocean	0.55 (5)	0.40 (4)	3.72 (22)	2.23 (13)	3.47 (31)	1.64 (15)	0.62 (6)	0.1 (1)	51	41
North Atlantic	−0.33 (−3)	−0.06 (−1)	−1.01 (−6)	−0.28 (−2)	−2.58 (−23)	−1.27 (−11)	−1.88 (−17)	−0.98 (−9)	52	59
Equatorial Atlantic	0.26(3)	0.25 (2)	1.02 (6)	0.78 (5)	−0.93 (−8)	−0.28 (−3)	−0.57 (−5)	−0.30 (−3)	56	10
South Atlantic	0.38 (4)	0.52 (5)	0.81 (5)	1.37 (8)	−0.5 (−5)	0.33 (3)	0.14 (1)	0.04 (0)	49	36
North Pacific	0.05 (0.5)	0.23 (2)	−0.29 (−2)	0.16 (1)	−2.10 (−19)	−0.64 (−6)	−0.35 (−3)	−0.07 (−1)	53	63
Equatorial Pacific	0.30 (3)	0.20 (2)	0.83(5)	0.55 (3)	−0.35 (−3)	−0.05 (0)	−0.6 (−5)	−0.26 (−2)	48	18
South Pacific	0.09 (1)	0.25 (3)	0.70 (4)	1.09 (6)	−1.07 (−10)	0.15 (1)	−0.82 (−7)	−0.43 (−4)	42	21
Global	0.14 (1)	0.21 (2)	0.62 (4)	0.54 (3)	0.39 (4)	0.26 (2)	0.11 (1)	−0.04 (−0.3)	28	11

[a]In parentheses are changes of wind speed ($ms^{-1} \times 10^{-2}$) and wave height ($m \times 10^{-2}$) with respect to the beginning of each period.
[b]STD in control run of 350 years.
[c]STD in historical run (1850–1950).

For the period of altimeter observations between 1985 and 2008 the WAM model shows generally consistent patterns in inter-annual variability, magnitude, and regional trends in wave height. Poor agreement between model and data in the Arctic Ocean is most likely due to very sparse coverage of hight latitudes by the altimeter. The WAM model calculates higher than observed by the altimeter wave heights in the low–wave regions such as the Equatorial Pacific and Atlantic. Despite a good agreement in trends direction, the model underestimates wave height in the North Atlantic compared to altimeter data. Best agreement in terms of both wave height magnitude and inter–annual trend is shown in the Southern Hemisphere, India Ocean, and North Pacific.

[11] Taking into account that the trends demonstrate higher decadal change rates over the last 6 decades than the first 10 decades in the historical period (Table 1), we conclude that four regions with the largest anomalies at the end of the 20th century in the wave height have appeared mostly during the last 6 decades. High positive wave height trends of 0.59×10^{-2} m, 2.23×10^{-2} m, 1.37×10^{-2} m, 1.09×10^{-2} m per decade in the Arctic Ocean, Southern Ocean, South Atlantic and Pacific respectively (Table 1) lead to positive anomalies of 0.03 m, 0.13 m, 0.08 m and 0.06 m (Figures 2d, 3a, 3g, 3h, and 3i). A negative anomaly in the North Atlantic indicates a decrease of wave height by −0.02 m (Figure 3b) which follows from a negative trend of -0.28×10^{-2} m per decade. The range of wave height changes for other regions is between 0.01 m (0.4%) in the North Pacific and 0.05 m (2.5%) in the Equatorial Atlantic. The projected most significant wind speed increase of 0.13 ms^{-1} (2.3%) and 0.22 ms^{-1} (2.5%) in the Arctic Ocean and Southern Ocean and a decrease of −0.06 ms^{-1} (−0.8%) in the North Atlantic (Figure 2a) results from large positive (negative) trends in the respective regions (Table 1). The range of wind changes for other regions (Figures 3c–3f, 3h,

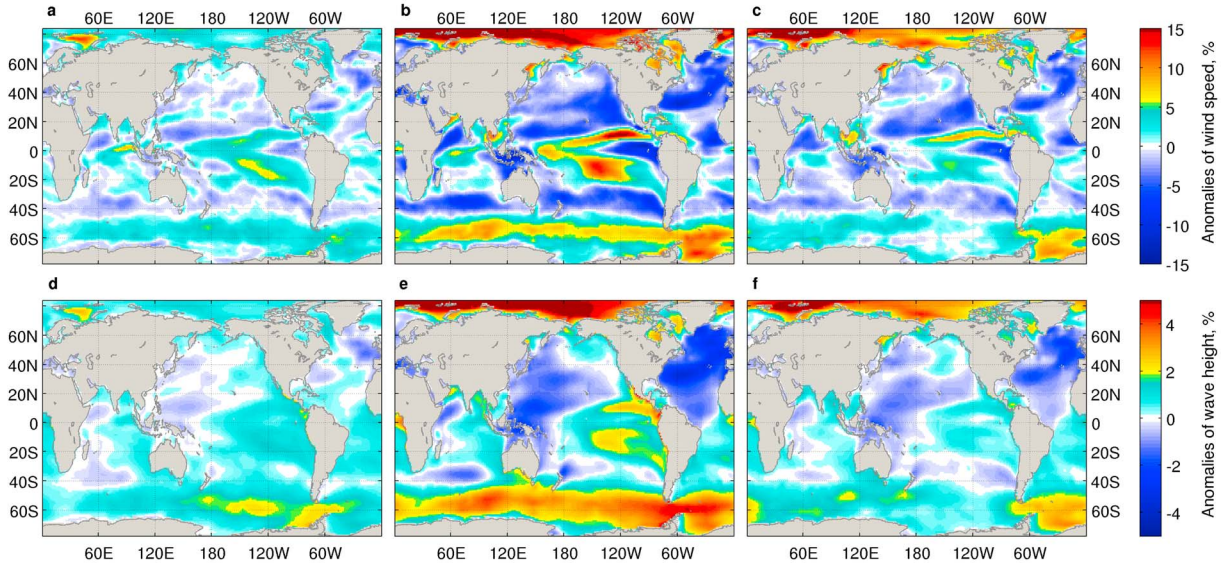

Figure 2. Anomalies (%) of (top) wind speed and (bottom) significant wave height, normalized to the reference period from 1850 to 1870: (a and d) for the historical period from 1989 to 1999; for the future period from 2090 to 2100 for scenarios (b and e) RCP8.5 and (c and f) RCP4.5.

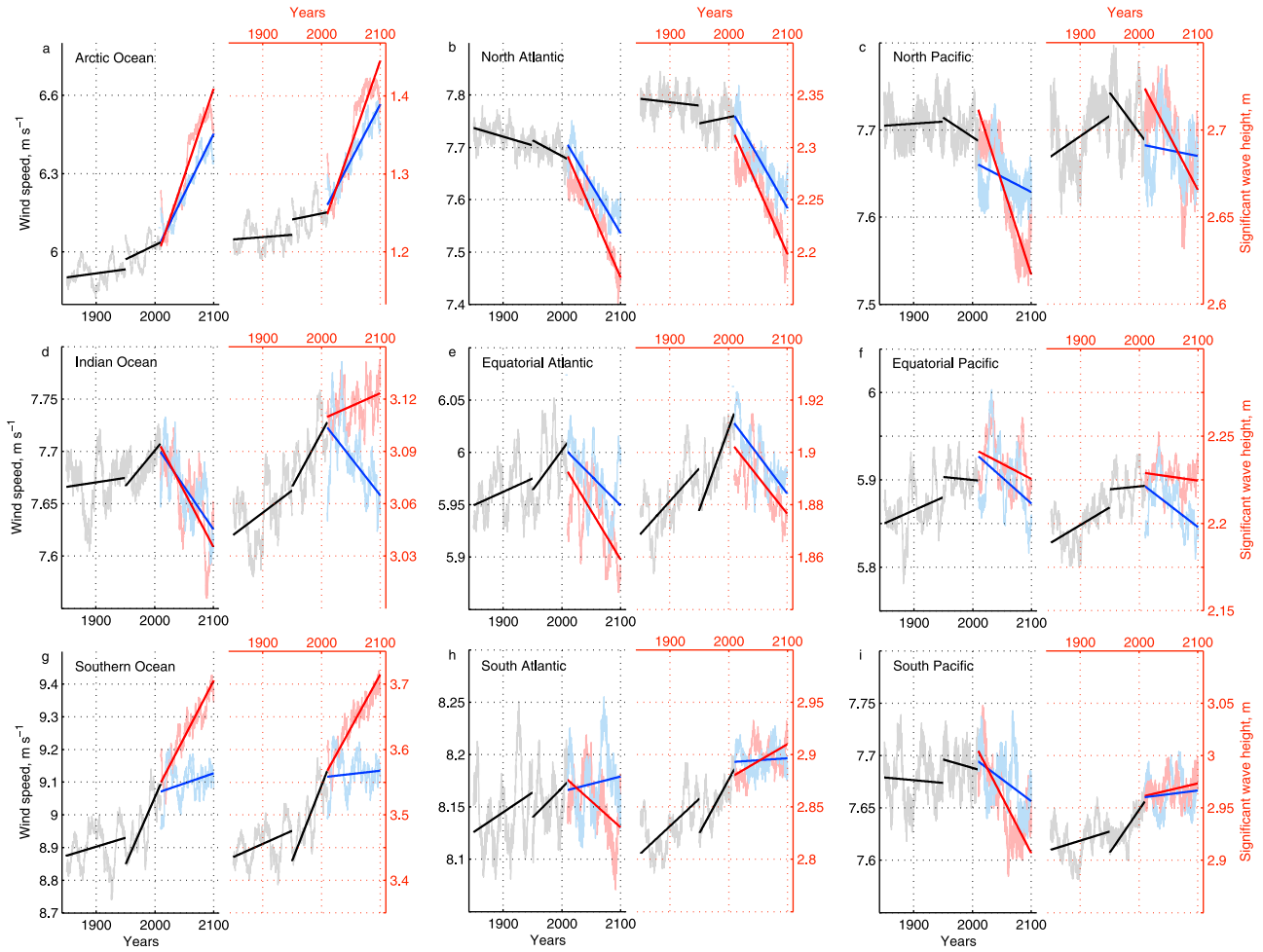

Figure 3. Simulated historical and future trends in the wind speed and significant wave height in the ocean basins of (a) Arctic Ocean, (b) North Atlantic, (c) North Pacific, (d) Indian Ocean, (e) equatorial Atlantic, (f) equatorial Pacific, (g) Southern Ocean, (h) South Atlantic, and (i) South Pacific: two historical sub–periods 1850–1950 and 1950–2010 (black lines); future period 2010–2100 for scenarios RCP8.5 (red line) and RCP4.5 (blue line). Shadowed lines are 10 year running mean values. Please note the different Y axis, wind speed on the left side (in black) and significant wave height on the right (in red).

and 3i) is from −0.2% in the North Pacific to 1.0% in the Equatorial Atlantic.

[12] In the RCP8.5 scenario, a substantial increase of the wind speed in polar regions, of 0.72 ms^{-1} (12.2%) and 0.54 ms^{-1} (6.0%) in the Arctic Ocean and Southern Ocean (see Figures 3a and 3g) is projected, which is in line with a continuous intensification of wind trends by the end of the 21st century up to 6.69×10^{-2} ms^{-1} per decade. The positive anomalies of wave height have been developed in magnitude to values of 0.23 m (18.8%) in the Arctic Ocean and 0.28 m (8.1%) in the Southern Ocean (Figures 2b and 2e). In the North Atlantic, the negative anomaly of wave height is evolving toward west and south and is decreasing towards −0.15 m (−6.3%). Large anomalies of wind speed and wave height are not necessary accompanied by significant changes over the entire period of simulation. Equatorial anomalies (Figures 2b and 2e) of wind speed (up to 15% in Pacific Ocean and −10% in Atlantic Ocean) and wave height (up to 3.5% in Pacific Ocean and −4% in Atlantic Ocean) are pronounced. However, over the entire period of 250 years the changes in the Equatorial Atlantic and Pacific range between −0.05 ms^{-1} (−0.9%) to 0.05 ms^{-1} (0.9%) for wind speed and between 0.01 m (0.4%) and 0.04 m (1.6%) for wave height, which is rather insignificant. In comparison to the RCP8.5 scenario, the main anomaly differences for the RCP4.5 scenario consist of a general decrease in magnitude (Table 1) and a shift of the positive anomaly maximum in the Southern Ocean from the Pacific towards the Atlantic (Figures 2c and 2f). The largest positive changes of 0.55 ms^{-1} (9.3%) wind speed and 0.17 m (14.2%) wave height are still predicted in the Arctic Ocean and in the Southern Ocean, where the values are 0.25 ms^{-1} (2.8%) wind speed and 0.13 m (3.8%) wave height. Negative changes of −0.20 ms^{-1} wind speed (−2.6%) and −0.10 m wave height (−4.5%) relative to the year 1850 are predicted for the North Atlantic. Reported regional changes are within the internal model variability except for the Arctic Ocean in RCP8.5 and RCP4.5 and for the Southern Ocean in RCP8.5 where the increase of wind speed exceed model variability (Table 1).

[13] For most ocean basins and for historical period and future scenarios RCP8.5 and RCP4.5, the wind speed and significant wave height are consistent in terms of direction

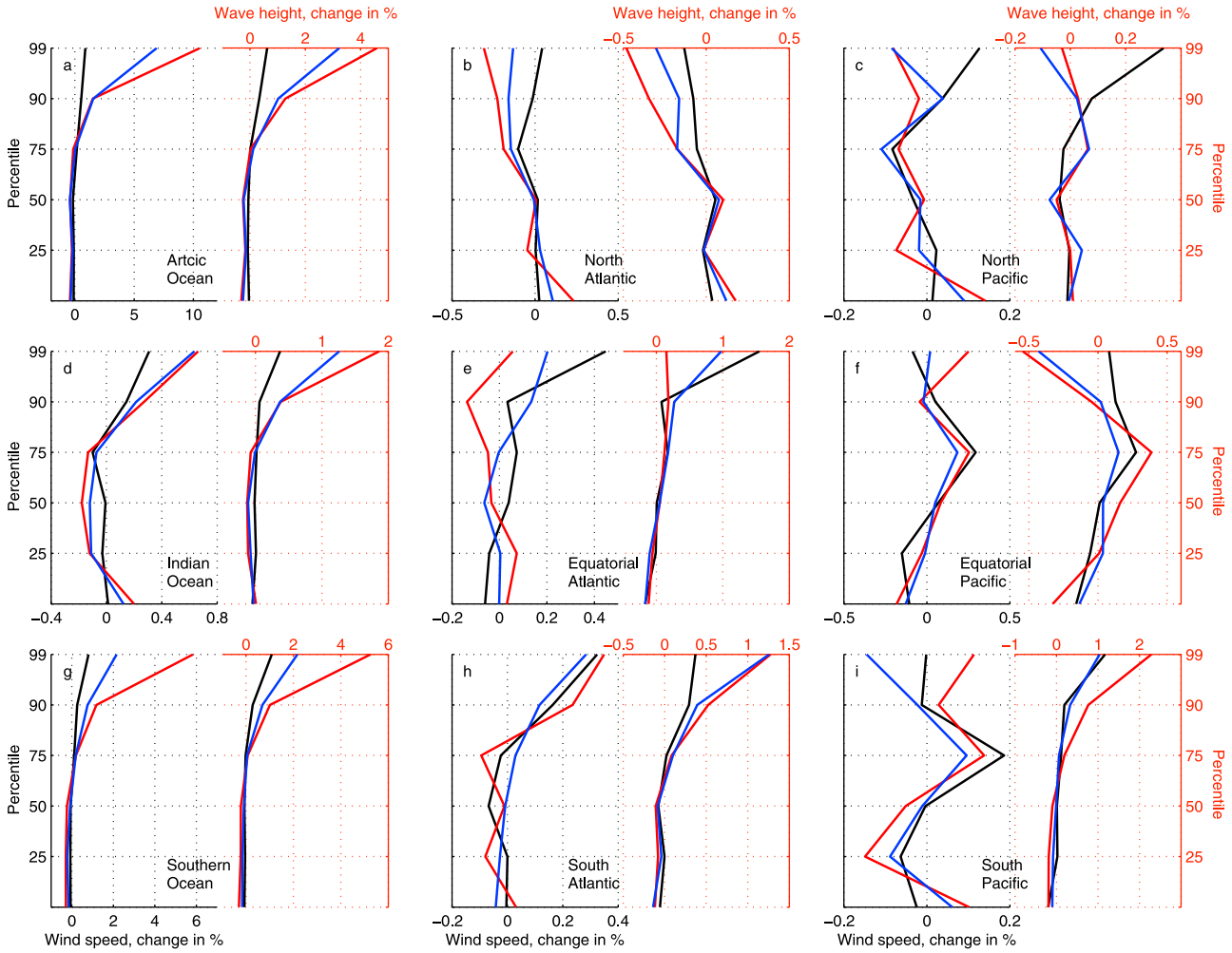

Figure 4. Changes in the probability of wind speed and wave height in ocean basins of (a) Arctic Ocean, (b) North Atlantic, (c) North Pacific, (d) Indian Ocean, (e) equatorial Atlantic, (f) equatorial Pacific, (g) Southern Ocean, (e) South Atlantic, and (f) South Pacific normalized to the historical period from 1850 to 1950: at present (black line); for the scenarios RCP8.5 (red line) and RCP4.5 (blue line). Please note the different Y-axis, wind speed on the left side (in black) and significant wave height on the right (in red).

of the change (Figure 3). However, swell propagation from the Southern Ocean to the open Indian Ocean, South Atlantic and Pacific leads to opposite signs of trends in wind speed and wave height. In these regions, swell developed in the Southern Ocean dominates local wind waves and increases the significant wave height despite a decrease of wind speed (Figures 3d, 3h, and 3i). This effect becomes smaller in the RCP4.5 scenario in the South Atlantic and Pacific and is not present in the Indian Ocean. Two regions are notable for their scenario dependent (RCP8.5 and RCP4.5) change in trend sign. In the South Atlantic (Figure 3h) the RCP8.5 trend in wind speed is projected negative, whereas the RCP4.5 trend is positive. In the Indian Ocean (Figure 3d) on the other hand, the RCP8.5 wave height trend is positive, whereas the RCP4.5 trend becomes negative, which is in line with a decrease of swell propagation from the Southern Ocean. This is also noticeable in the South Atlantic and Pacific (Figures 3h and 3i).

[14] We classified wind and waves conditions in terms of low, medium, above medium, high, very high and extreme values using the 25, 50, 75, 90 and 99 percentiles as threshold values between the states. These percentiles have been calculated from the reference period of the first 100 years of the historical run. We estimated the probability density function of wind speed and wave height by a kernel density estimation, calculating the probability for each interval limited by percentiles. The changes of probability compared to present (2010) and for the future scenarios (2010–2100) were normalized to the reference period (Figure 4). In the polar regions, a clear tendency for an probability increase of very high and extreme values of wind speed and wave height is indicated (Figures 4a and 4g) by maximum of 10.5% for the wind speed and 4.6% for the wave height in the Arctic Ocean and by 5.8% and 5.2% in the Southern Ocean, respectively. In the Indian Ocean, low and high to extreme values become most probable at the end of 2100 reaching values of 0.7% for RCP4.5 wind speed and 1.9% for RCP8.5 (Figure 4d). An probability increase of very high and extreme values of wind speed (0.4%) and wave height (2.3%) is notable in Equatorial and South Atlantic and in the South Pacific (Figures 4e, 4h, and 4i). In the North Atlantic, extremes are less probable and for both scenarios the probability for low values is higher in the future (Figure 4b). The changes in the North Pacific are negligibly small (Figure 4c). The mid–range of the wave height spectrum in the Equatorial Pacific becomes more

probable, which is accompanied by an probability decrease of low and extreme values (Figure 4f).

5. Concluding Remarks

[15] The future wave climate (Table 1) shows that at the end of the 21th century the globally averaged monthly wind speed will continue to increase by 0.04 m (0.39×10^{-2} ms^{-1} per decade) in the RCP8.5 scenario and by 0.01 m (0.1×10^{-2} ms^{-1} per decade) in the RCP4.5 scenario. The globally averaged monthly significant wave height is projected to increase by 0.02 m (0.26×10^{-2} m per decade) at the end of the 21th century projected in the RCP8.5 scenario, but to decrease by -0.04 m (-0.3×10^{-2} m per decade) in the RCP4.5 scenario. The magnitude of changes varies strongly from region to region, with a maximum increase of 0.6 ms^{-1} (10.0% relative to present) and 0.3 ms^{-1} (3.4%) in wind speed and 0.2 m (15.7%) and 0.15 m (4.1%) in wave height in the Arctic Ocean and Southern Ocean in the RPC8.5 scenario. The decreases of -0.23 ms^{-1} (-3.0%) and -0.19 ms^{-1} (-2.4%) in the wind speed and -0.11 m (-4.9%) and -0.06 m (-2.1%) in wave height are projected in the North Atlantic and Pacific. For several regions (Indian Ocean, Equatorial and South Atlantic and Pacific) a change in sign of the wind speed trend is projected for the future, if compared to the present. The sign of the wave height trend is only changing in Equatorial Atlantic, the Pacific and North Pacific. Globally and for the most of ocean basins (except Arctic and Southern Ocean for the wind speed) the predicted trends are still inside the margin of natural variability as estimated from the 350 years control simulation under pre-industrial conditions for wind speed and from the historical run for wave height. However, a probability increase of very high and extreme values of wind speed and wave height is projected for both scenarios in the Southern hemisphere, Arctic and Indian Ocean. In the North and Equatorial Atlantic and in the Pacific these probabilities are decreasing, in line with a probability increase of low to medium winds and waves.

[16] **Acknowledgments.** Authors would like to thank T. Ilina and M. Giorgetta from the Max Planck Institute for Meteorology, A. Karpechko from the Finnish Meteorological Institute and J. W. Nielsen from the Danish Meteorological Institute for comments and many helpful discussions during this study and S. Zieger from the Swinburne University of Technology for the altimeter data set. This work was partly funded by the EU Interreg IV B project #056 BaltAdapt, the European Commission's 7th Framework Programme, under grant agreement 226520, COMBINE project and the Centre for Regional Change in the Earth System – CRES, founded by the Danish Council of Strategic Research.

[17] The authors and the Editor thank anonymous reviewers for assisting in the evaluation of this paper.

References

Allan, J., and P. Komar (2000), Are ocean wave heights increasing in the eastern North Pacific?, *Eos Trans. AGU*, *81*(47), 561–567.

Amante, C., and B. Eakins (2009), Etopo1 1 arc-minute global relief model: Procedures, data sources and analysis, *NOAA Tech. Memo. NESDIS NGDC-24*, 25 pp., NOAA, Silver Spring, Md.

Babanin, A. V. (2006), On a wave-induced turbulence and a wave-mixed upper ocean layer, *Geophys. Res. Lett.*, *33*, L20605, doi:10.1029/2006GL027308.

Babanin, A. V., A. Ganopolski, and W. R. C. Phillips (2009), Wave-induced upper-ocean mixing in a climate model of intermediate complexity, *Ocean Modell.*, *29*, 189–197.

Bacon, S., and D. J. T. Carter (1991), Wave climate changes in the North Atlantic and North Sea, *Int. J. Climatol.*, *11*, 545–558.

Carter, D., and L. Draper (1988), Has the north-east Atlantic become rougher?, *Nature*, *332*, 494.

Cox, A. T., and V. R. Swail (2001), A global wave hindcast over the period 1958–1997: Validation and climate assessment, *J. Geophys. Res.*, *106*, 2313–2329.

Donelan, M., W. Drennan, and K. Katsaros (1997), The air-sea momentum flux in conditions of wind sea and swell, *J. Phys. Oceanogr.*, *27*, 2087–2099.

Hazeleger, W., et al. (2012), EC-Earth v2.2: Description and validation of a new seamless Earth system prediction model, *Clim. Dyn.*, doi:10.1007/s00382-011-1228-5, in press.

Intergovernmental Panel on Climate Change (2007), *Climate Change 2007: The Physical Science Basis. Contribution of Working Group I to the Fourth Assessment Report of the Intergovernmental Panel on Climate Change*, edited by S. Solomon et al., Cambridge Univ. Press, Cambridge, U. K.

Levitus, S., et al. (2006), *World Ocean Database 2005*, 199 pp., NOAA, Silver Spring, Md.

Lorenz, D. J., and E. T. DeWeaver (2007), Tropopause height and zonal wind response to global warming in the IPCC scenario integrations, *J. Geophys. Res.*, *112*, D10119, doi:10.1029/2006JD008087.

Qiao, F., and C. J. Huang (2012), Comparison between vertical shear mixing and surface wave-induced mixing in the extratropical ocean, *J. Geophys. Res.*, *117*, C00J16, doi:10.1029/2012JC007930.

Marshall, G. (2003), Trends in the southern annular mode from observations and reanalyses, *J. Clim.*, *16*(24), 4134–4143.

Pleskachevsky, A., M. Dobrynin, H. Guenther and E. Stanev (2011), Turbulent mixing due to surface waves indicated by remote sensing of suspended particulate matter and its implementation into coupled modeling of waves, turbulence and circulation, *J. Phys. Oceanogr.*, *41*(4), 708–724.

Shindell, D. T. and G. A. Schmidt (2004), Southern Hemisphere climate response to ozone changes and greenhouse gas increases, *Geophys. Res. Lett.*, *31*, L18209, doi:10.1029/2004GL020724.

Taylor, K. E., R. J. Stouffer, and G. A. Meehl (2012), An overview of CMIP5 and the experiment design, *Bull. Am. Meteorol. Soc.*, *93*, 485–498, doi:10.1175/BAMS-D-11-00094.1.

van Vuuren, D., et al. (2011), The representative concentration pathways: An overview, *Clim. Change*, *109*, 5–31.

Wamdi Group (1988), The WAM model—A third generation ocean wave prediction model, *J. Phys. Oceanogr.*, *18*(12), 1775–1810.

Wang, X., and V. Swail (2006), Climate change signal and uncertainty in projections of ocean wave heights, *Clim. Dyn.*, *26*, 109—126.

Woollings, T., J. Gregory, J. Pinto, M. Reyers, and D. Brayshaw (2012), Response of the North Atlantic storm track to climate change shaped by ocean–atmosphere coupling, *Nat. Geosci.*, *3*, 313–317.

Yin, J. H. (2005), A consistent poleward shift of the storm tracks in simulations of 21st century climate, *Geophys. Res. Lett.*, *32*, L18701, doi:10.1029/2005GL023684.

Young, I. R., S. Zieger, and A. V. Babanin (2011), Global trends in wind speed and wave height, *Science*, *332*(6028), 451–455, doi:10.1126/science.1197219.

Zieger, S., J. Vinoth, and I. Young (2009), Joint calibration of multiplatform altimeter measurements of wind speed and wave height over the past 20 years, *J. Atmos. Oceanic Technol.*, *26*(12), 2549–2564.